

Antenna Array Pattern Nulling by Phase Perturbations using Modified Differential Evolution Algorithm



S. Venkata Rama Rao¹, A. Mallikarjuna Prasad², Ch. Santhi Rani³

¹Research scholar, Department of ECE, JNTUK, Kakinada, India.

²Professor of ECE, University College of Engineering, JNTUK, Kakinada, India.

³Professor of ECE, USHA RAMA College of Engineering and Technology, Telaprolu, India.

ABSTRACT

In this paper, a modified differential evolution algorithm (MDE) is proposed for inserting asymmetrical nulls in various linear antenna array (LAA) configurations. The proposed algorithm optimizes the phase excitations of individual array elements for keeping nulls in any interfering direction. The MDE algorithm replaces the mutation factor in traditional differential evolution algorithm with normal mutation. Simulation results of several Taylor Profile Amplitude Distributed (TPAD) linear antenna array configurations are considered for keeping nulls at any prescribed direction.

Key words: Asymmetrical nulls, mutation factor, MDE, normal distribution, TPAD linear array.

1. INTRODUCTION

The electromagnetic Pollution is increasing day by day because of the growing modern communication systems. In these polluted environments, placing nulls in unwanted interfering directions by keeping low side lobe levels is a very important factor [1-2]. In array pattern synthesis problems null steering with deep nulls can be achieved by excitation of phase only, amplitude only, both amplitude and phase and position-only methods. Each of the methods stated above has its own advantage and disadvantage. Moreover, in practice since the phases of the array elements can be controlled by a simple phase shifters, array elements phase control is much simpler than amplitude control. In mobile communication antenna arrays are required not to radiate power in particular directions. Hence the radiated power along these directions is negligible. This is achieved by placing nulls along these directions in the antenna array pattern.

In communication systems such as cellular and radar systems around the main lobe, several nulls have to be placed asymmetrically. The position only and amplitude only optimization methods are incapable to place the asymmetrical nulls in the

interfering directions. However, the phase-only optimization techniques can keep asymmetrical nulls effectively around the main beam.

In literature, several global optimization methods such as the genetic algorithm [3-4], particle swarm optimization [1,5], simulated annealing [6], ant colony algorithm [7], invasive weed optimization [8], modified touring ant colony algorithm [9], cat swarm optimization [10] and differential evolution algorithm [11] are successfully applied than conventional optimization techniques in LAA pattern nulls. The proposed MDE algorithm optimizes the phase excitation of the individual array elements to keep the nulls in the directions of interference.

The rest of the paper is organized as follows. Section II presents the LAA configuration and problem formulation, section III discusses the DE algorithm, section IV discusses the MDE algorithm, simulation results in section V and conclusion part is present in section VI.

2. PROBLEM FORMULATION

We considered the linear antenna array (LAA) with $2M$ isotropic radiators symmetrically placed on the x axis [12]. The LAA geometry is shown in figure 1.

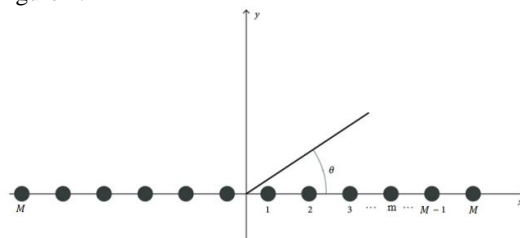


Figure 1: Geometry of $2M$ elements symmetrically placed linear antenna array along x-axis

The far field array factor (AF) of symmetrically placed linear array can be expressed as [2]

$$AF(\theta) = \sum_{m=1}^M A_m e^{jkd_m \sin \theta} \quad (1)$$

Where,

θ = Azimuth angle,

$k = 2\pi/\lambda$ is wave number of wave,
 d_m = Position of the m^{th} array element,
 $A_m = I_m e^{j\phi_m}$.
 I_m = Amplitude of the m^{th} element with phase ϕ_m

The problem statement is defined as to optimize the sidelobe levels and to control null positions of TPAD antenna elements.

The fitness function for side lobe level (SLL) suppression is [1],

$$f_{SLL\ suppression} = \sum_i \frac{1}{\Delta\theta_i} \int_{\theta_{li}}^{\theta_{ui}} |AF(\theta)|^2 d\theta \quad (2)$$

Where θ_{li} and θ_{ui} are the spatial regions corresponding to low sidelobe levels and $\Delta\theta_i = \theta_{ui} - \theta_{li}$

The fitness function for Null control is [1],

$$f_{Null\ control} = \sum_k |AF(\theta_k)|^2 \quad (3)$$

The fitness function (FF) for achieving both SLL suppression and null control is obtained by adding above two equations given by [1],

$$FF = f_{SLL\ suppression} + f_{Null\ control} \quad (4)$$

$$FF = \sum_i \frac{1}{\Delta\theta_i} \int_{\theta_{li}}^{\theta_{ui}} |AF(\theta)|^2 + \sum_k |AF(\theta_k)|^2 \quad (5)$$

Where, θ_k values are direction of nulls in the desired directions.

3. DIFFERENTIAL EVOLUTION (DE)

In recent years the DE algorithm (proposed by Storn and Price) and its variants are successfully applied to LAA synthesis problems. The DE algorithm is a simple and straightforward method to apply compared to other evolutionary algorithms (EAs). In the DE algorithm without having prior knowledge about the optimum solution, the initial population is considered within upper and lower boundary constraints is an important step. The initial population in the DE is represented by NP and the number of optimized parameters to be taken as D. We can denote the individual population in g^{th} generation by,

$$X_{i,g} = \{x_{1,i,g}, x_{2,i,g}, \dots, x_{d,i,g}\} \quad (6)$$

After the initialization process, the differential mutation is applied and then crossover and selection operations are applied.

(a) Mutation Operation: The next step after initialization is to create donor vector $u_{i,g}$. DE algorithm uses different mutant strategies to create donor vector. Among these strategies, we consider a particular mutation strategy DE/best/1 for generating donor vector $u_{i,g}$.

$$u_{i,g} = X_{best,g} + F(X_{r1,g} - X_{r2,g}) \quad (7)$$

Where, $r1$ and $r2$ are integers in the range [1, NP], $X_{best,g}$ is the best fitness vector corresponding to g^{th} generation in the population and F is scaling factor.

(b) Crossover Operation: After the mutation process, DE generates a trail vector $V_{i,g}$ using the crossover operation. In this paper among the two crossover methods exponential and uniform crossover, we focus on the mostly used uniform crossover method. By using uniform crossover strategy the trail vector can be obtained by,

$$V_{j,i,g} = \begin{cases} u_{j,i,g} & \text{if } rand(0,1) \leq C_r \text{ or } j = j_{rand} \\ X_{j,i,g} & \text{otherwise} \end{cases} \quad (8)$$

Where C_r is the crossover factor in the range [0, 1], $X_{j,i,g}$ is the target vector, $u_{j,i,g}$ is the corresponding mutant vector and j_{rand} is the random number in the range [1, D].

(c) Selection: After the crossover operation the selection process compares the fitness of the trail vector $V_{j,i,g}$ with corresponding target vector $X_{j,i,g}$. Among these two the smallest fitness vector survives to the next generation $g+1$. The selection process can be expressed as,

$$X_{i,g+1} = \begin{cases} u_{j,i,g} & \text{if } f(V_{i,g}) < f(X_{i,g}) \\ X_{j,i,g} & \text{otherwise} \end{cases} \quad (9)$$

4. MDE ALGORITHM

The performance of the DE algorithm mostly depends on evolutionary operations mutation, crossover, and selection. Many researchers are trying to improve the DE algorithm by adopting modifications in these evolutionary operators. Among these operators mutation is an important factor to balance global exploration and local exploitation abilities. In this paper, MDE is proposed by adopting the normal mutation operator in the mutation part of the traditional DE.

The probability density function of the normal distribution can be expressed as [2]

$$f_{normal}(x; \mu, \sigma^2) = \frac{1}{\sqrt{2\pi\sigma^2}} e^{-\frac{(x-\mu)^2}{2\sigma^2}} \quad (10)$$

Where, μ , σ and σ^2 are mean, standard deviation and variance of the distribution

The normal mutation is mathematically expressed as,

$$g_i^{t+1} = g_i^t + \sigma N(0,1) \quad (11)$$

For the normal distribution $N(0, 1)$ in the above equation, the mean is zero and the standard deviation is 1.

In MDE modified mutation vector to create a donor, vector is defined as [2]

$$U_{i,g} = X_{best,g} + [F * X_{best,g} * N(0,1)] \quad (12)$$

Where F is the mutation scaling factor adjusts the step size for the normal distribution.

5. NUMERICAL EXPERIMENTS

In this paper, MDE is used to synthesize linear arrays of 10 elements and 28 elements with element spacing $\lambda/2$ and the operating frequency is 300MHz. The simulations are carried out by neglecting the mutual coupling effect between array elements. In the unwanted interfering directions deep nulls are placed by optimizing the phase excitations of each array element. Here by using a 30dB Taylor Profile Amplitude Distribution (TPAD) the amplitudes of every array element is obtained. In all the experiments for 10 elements the

first null beam width (FNBW) is kept constant at 35° with tolerance of $\pm 5\%$, which is the FNBW of 10 element of non optimized TPAD.

The MDE algorithm is computed on MATLAB R2015a environment and a PC operating 1.7 GHz with 4GB RAM. The parameter assumed for MDE algorithm are number of population $N_p=50$, crossover rate (Cr) is 0.5 and scaling factor (SF) is 0.9. For computing the radiation pattern the number of azimuth angles consider are 720 in the angular region of -90° to 90° . The obtained optimized values of phase excitation with MDE algorithm are tabulated in Table 1.

Table 1: Optimized phase excitations of TPAD LAA with MDE algorithm for null placing

Example	Number of Array Elements	MDE Optimized Phase Excitations (in deg)	Nulls at Position (in deg)
1	10 Elements	-0.3722, 0.0551, 0.0461, 0.0257, 0.0133, -0.0209, -0.0299, -0.1096, -0.0674, 0.0415	$24^\circ, 33^\circ$
2		-2.9991, -3.0235, 3.0389, -3.0690, 3.1409, -3.1410, 3.0607, 3.1355, 2.9220, 2.7831	$-33^\circ, -58^\circ$
3		0.0013, -2.5568, -3.1207, -3.1191, 3.1416, -3.0563, 3.0037, -3.1041, -2.7470, 3.1177	$-32^\circ, 42^\circ$
4		-0.2016, -0.1195, -0.2607, -0.3607, -0.4091, -0.3616, -0.3444, -0.3621, -0.4236, -0.2407	$29^\circ, 35^\circ, 52^\circ$
5	28 Elements	-1.1594, 0.2514, 0.2658, -0.2086, -0.0239, -0.2920, -0.1605, -0.2841, -0.1455, -0.1081, -0.0720, -0.0631, 0.0385, 0.0851, 0.1026, 0.1265, 0.2132, 0.1891, 0.1955, 0.1771, 0.1693, 0.1773, -0.0092, -0.0128, -0.0417, -1.0938, 0.4114, -0.5770	$22^\circ, 32^\circ$
6		-0.4499, 0.3362, -0.2982, -0.2902, 0.0115, -0.5514, -0.0411, -0.0943, -0.0685, -0.1456, -0.2445, -0.3051, -0.3529, -0.3692, -0.2676, -0.2733, -0.1960, -0.2701, -0.1943, -0.0945, -0.0699, 0.3154, 0.254, 0.0273, 0.2841, -0.0522, 0.7565, 0.2916	$20^\circ, 22.5^\circ, 32^\circ$
7		0.0484, 0.0111, -0.1394, 0.0430, 0.0927, -0.0160, -0.0070, 0.1057, 0.0320, -0.0367, -0.0249, 0.0109, -0.0069, 0.0116, -0.0115, -0.0202, 0.0048, -0.0466, -0.0282, -0.0152, 0.0482, 0.0019, -0.0194, -0.0121, -0.0616, -0.0312, -0.0670, 0.1233	$-21^\circ, 25^\circ, 52^\circ$

Design Example 1: 10 elements TPAD linear array with two nulls positioned at 24° and 33°

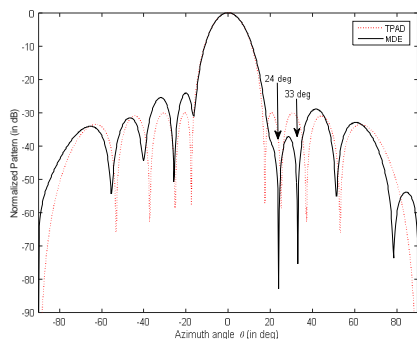


Figure 2: Normalized array Pattern for position only optimized 10 elements TPAD linear array with double imposed nulls at 24° and 33°

The first example refers to a 10 element TPAD synthesis with two nulls positioned at 24° and 33° . In this simulation phase excitations of individual array elements are controlled by MDE algorithm by maintaining the Taylor profile for the amplitudes of individual array elements. The corresponding

normalized radiation pattern and convergence curves of the fitness function respectively have shown in figure 2 and 3. During optimization without changing the excitation amplitudes, the excitation phases are optimized with MDE algorithm.

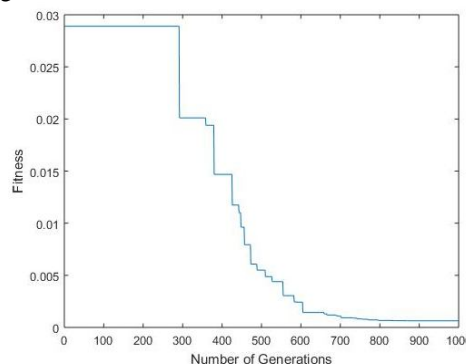


Figure 3: Convergence plot for 10 elements TPAD linear array with nulls at 24° and 33°
Design Example 2: 10 elements TPAD linear array with two nulls positioned at $-33^\circ, -58^\circ$.

The second example shows the synthesized pattern with two nulls placed at negative azimuth angles in the directions of interference signals. The normalized array pattern with nulls at -33° and -58° is shown in figure 4 and figure 5 presents corresponding convergence curve. From figure 4 it is evident that the MDE algorithm can keep nulls as deep as -70dB along null positions.

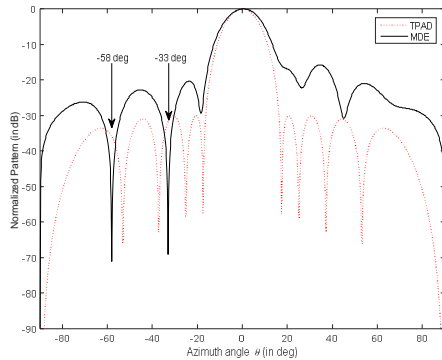


Figure 4: Normalized array Pattern for position only optimized 10 elements TPAD linear array with nulls at negative azimuth angles -33° and -58°

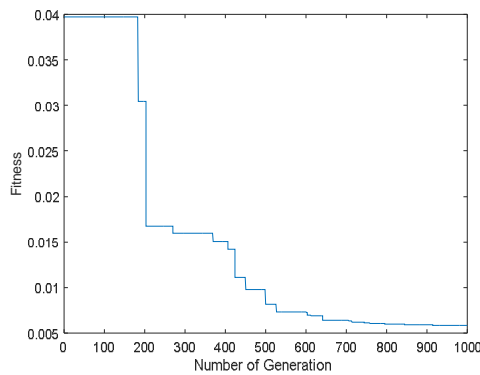


Figure 5: Convergence plot for 10 elements TPAD linear array with azimuth angles -33° and -58°

Design Example 3: The 10 elements TPAD linear array with nulls positioned around the main beam at -32° and 42° .

Figure 6 shows the synthesised pattern with two nulls imposed at -32° and 42° by optimizing the TPAD array phase excitations by fixing the main beam position at 0° and the corresponding convergence function is shown in figure 7. From figure 6 it is noted that nulls obtained at the interference directions are as deep as -65dB . Hence MDE algorithm can also place deep nulls even the nulls are positioned at positive and negative azimuth angles.

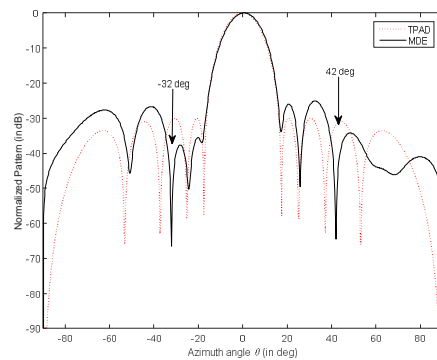


Figure 6: Normalized array Pattern for position only optimized 10 elements TPAD linear array with nulls on both sides of main beam at azimuth angles -32° and 42° .

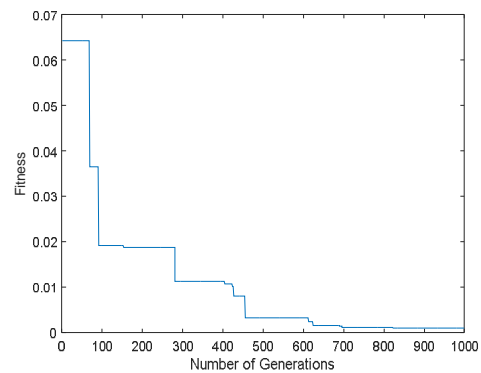


Figure 7: Convergence plot for 10 elements TPAD linear array with nulls on both sides of main beam at azimuth angles -32° and 42° .

Design Example 4: 10 elements TPAD linear array with triple imposed nulls at 29° , 35° and 52° .

In the fourth example, three nulls are placed at 29° , 35° and 52° . The optimized pattern with imposed nulls is shown in figure 8 and the convergence curve is shown in figure 9. From the figure 8 nulls are as deep as -75 are obtained.

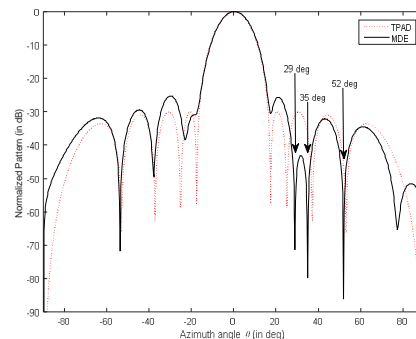


Figure 8: Normalized array Pattern for position only optimized 28 elements TPAD linear array with triple imposed nulls at 29° , 35° and 52°

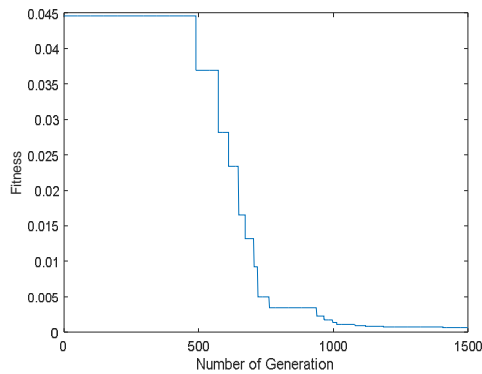


Figure 9: Convergence plot for 10 elements TPAD LAA with triple imposed nulls at 29° , 35° and 52°

Design Example 5: 28 elements TPAD linear array with double imposed at 22° and 32° .

By keeping the main lobe direction at 0° multiple nulls are placed at 22° and 32° . Radiation pattern of 28 element TPAD phase optimized linear array is shown in figure 10. And corresponding convergence curve is shown in figure 11. From figure 10 it is observed that null depths achieved with this configuration are as depth as -90 .

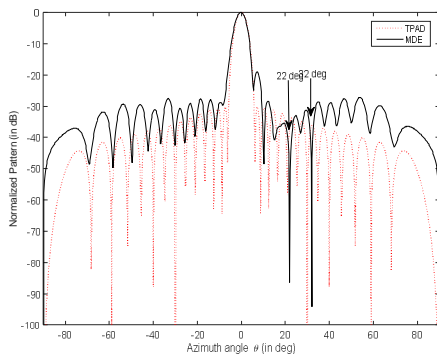


Figure 10: Normalized array Pattern for position only optimized 28 elements TPAD LAA with double imposed nulls at 22° and 32°

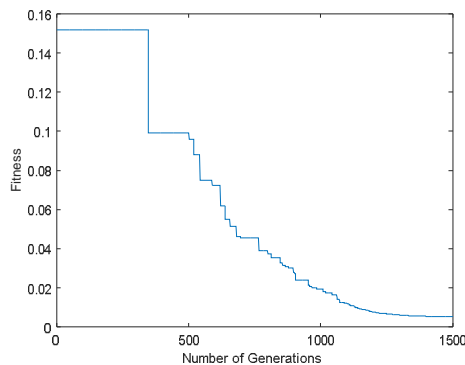


Figure 11: Convergence plot for 28 elements TPAD LAA with imposed nulls at 22° and 32°

Design Example 6: Radiation pattern of 28 elements TPAD LAA with triple imposed null at 20° , 22.5° and 32° .

In the sixth example the normalized far field pattern of 28 element TPAD LAA with phase only excitation places nulls at prescribed directions

20° , 22.5° and 32° as shown in figure 12 and corresponding convergence graphs is shown in figure 13. From the figure 12 it is noted that the nulls as deep as -80 are obtained at the direction of interferes.

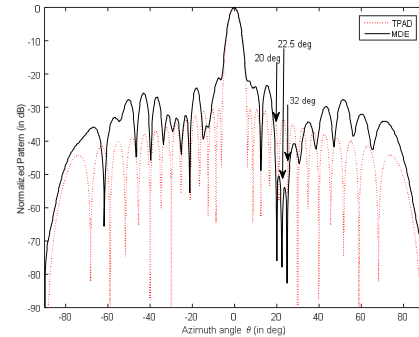


Figure 12: Normalized array Pattern for position only optimized 28 elements TPAD linear array with triple imposed nulls at 20° , 22.5° and 32°

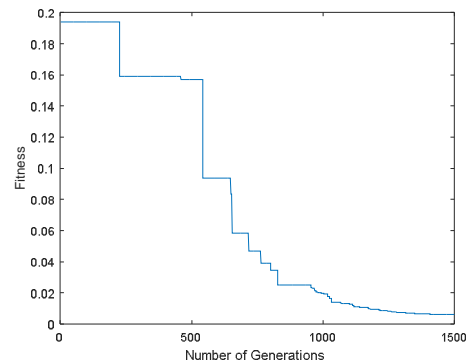


Figure 13: Convergence plot for 28 elements TPAD LAA with triple imposed nulls at 20° , 22.5° and 32°

Design Example 7: Radiation pattern of 28 elements TPAD LAA with triple imposed nulls at -21° , 25° , and 52° .

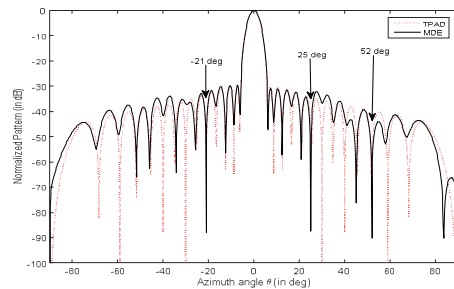


Figure 14: Normalized array Pattern for position only optimized 28 elements TPAD linear array with triple imposed nulls on both sides of main beam at -21° , 25° and 52°

Normalized far field pattern of 28 elements TPAD LAA with triple imposed nulls at -21° , 25° , and 52° . Figures 14 and 15 shows radiation pattern and corresponding convergence plot with nulls around the main beam at 21° , 25° , and 52° . In this case the imposed nulls are as deep as -90° .

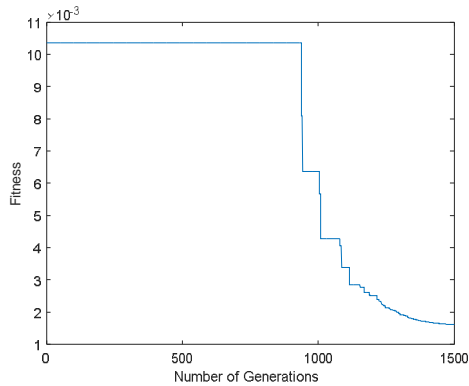


Figure 15: Convergence plot for 28 elements TPAD linear array with triple imposed nulls on both sides of main beam at -21° , 25° and 52°

The above seven examples demonstrate that by MDE algorithm for phase only optimization creates pattern nulls in the specified interfering directions. This is also true for the closely spaced null or the nulls are close to main beam.

6. CONCLUSION

The TPAD linear antenna array pattern synthesis with nulls by optimizing the phase only of array elements based on the modified DE algorithm is presented in the paper. It is noted that the MDE algorithm for phase only optimization allows null in any undesired interfering directions. It also true for the asymmetrical nulls placed around the main beam. The obtained results show that MDE algorithm for position only optimization has a fast convergence rate and global search capability.

REFERENCES

- [1] M. Khodier and C. Christodoulou, **Linear Array Geometry Synthesis with Minimum Sidelobe Level and Null Control Using Particle Swarm Optimization**, *IEEE Trans. Antennas Propag.*, vol. 53, no. 8, Aug. 2005, pp. 2674-2679. <https://doi.org/10.1109/TAP.2005.851762>
- [2] S.V.Rama Rao, A.M.Prasad, Ch.Santhi Rani, **Unequally Spaced Linear Antenna Array Synthesis with Minimum Side Lobe Levels Using Modified Differential Evolution Algorithm**, *International Journal of Innovative Technology and Exploring Engineering (IJITEE)*, Vol 8, 2019, pp. 908-914.
- [3] R. L. Haupt, **Phase-only Adaptive Nulling with a Genetic Algorithm**, *IEEE Trans. Antennas Propag.*, vol. 45, Aug. 1997, pp. 1009-1015. <https://doi.org/10.1109/8.585749>
- [4] D.W. Boeringer and D. H. Werner, **Particle swarm optimization versus genetic algorithms for phased array synthesis**, *IEEE Trans. Antennas Propag.*, vol. 52, no. 3, pp. 771-779, Mar. 2004. <https://doi.org/10.1109/TAP.2004.825102>
- [5] L Pappula, D Ghosh, **Linear antenna array synthesis for wireless communications using**

particle swarm optimization, *Proceedings of IEEE International conference on advanced communications technology*, pp. 780-783, January 2013.

[6] V.Murino, A.Truccho, CS. Regazzoni, **Synthesis of unequally spaced arrays by simulated annealing**, *IEEE transaction on Signal Processing*, vol. 44, pp. 119-123, 1996.

<https://doi.org/10.1109/78.482017>

[7] Eva Rajo-Iglesias and Oscar Quevedo Tteruel., **Linear array synthesis using an Ant colony optimization-based algorithm**, *IEEE transactions on antennas and propagation*, vol. 49, no. 2, 2007, pp. 70-79.

<https://doi.org/10.1109/MAP.2007.376644>

[8] L Pappula, D Ghosh, **Antenna Array Pattern Nulling by Phase Perturbations using Invasive Weed Optimization**, *9th International Radar Symposium India (IRSI - 13)*, 2013.

[9] D.Karaboga, K.Guney, A.Akdagli, **Antenna array pattern nulling by controlling both amplitude and phase using modified touring ant colony optimization algorithm**, *International Journal of Electronics*, vol. 91, 2004, pp. 241-251. <https://doi.org/10.1080/00207210410001690638>

[10] L Pappula, D Ghosh, **Linear antenna array synthesis using cat swarm optimization**, *AEU-International Journal of Electronics and Communications*, vol.68, 2014, pp.540-549.

<https://doi.org/10.1016/j.aeue.2013.12.012>

[11] S.Yang, Y B Gan, A Qing, **Antenna-array pattern nulling using a differential evolution algorithm**, *International Journal of RF Microwave CAE*, vol. 14, 2004; pp. 57-63.

<https://doi.org/10.1002/mmce.10118>

[12] S.V.Rama Rao, A.M.Prasad, Ch. Santhi Rani, **Direction of Arrival Estimation of Uncorrelated Signals Using Root-MUSIC Algorithm for ULAs and UCAs**, *International Journal of Engineering & Technology (IJET)*, Vol 7, 2018, pp. 398-401.

<https://doi.org/10.14419/ijet.v7i4.36.23813>